Final Technical Report, F62562-00M9154

Tbit/s optical switches and logic gates: Towards tunable operation near 1.55 μm

Irina Talanina

Department of Theoretical Physics
Research School of Physical Sciences and Engineering
Australian National University, Canberra ACT 0200, Australia

Abstract

In the performed research work, wavelength dependence (effects of detuning) and a possibility of tunable operation of the resonant soliton switches and logic gates have been investigated. A dramatic difference in the response to detuning between the semiconductor NLDC and atomic SIT-soliton NLDC has been revealed. A typical tunability range of a model resonant soliton NLDC has been assessed quantitatively and compared with a requirement for the device operating spectral range in WDM systems (applied by the gain bandwidth of erbium-doped fiber amplifiers). Extensive literature search has been performed to identify semiconductor materials which are suitable for implementation of the resonant soliton switches capable of tunable operation near the optical communication wavelength (1.55 μm). A number of semiconductor systems with the required excitonic absorption features have been selected including InGaAs/InAlAs MQW, InGaNAs/GaAs MQW, InGaAs/InP MQW, InGaAsP/InP MQW and GaSb/AlGaSb MQW structures. Modeling of operation of InGaAs/InAlAs MQW NLDC near 1.55 μm has been performed; a tunability range of about 25 nm and a mean switching contrast ratio of 20:1 within this range have been demonstrated numerically. A new device design has been suggested as a possible way to substantially increase the device tunability range. In the new design, semiconductor quantum-dot-doped glass has been used as a material for the constituent waveguides of NLDC. The use of PbS quantum dots has lead to a broader device tunability range (at least, 65 nm) near 1.55 μm.

REPORT DOCUMENTATION PAGE

Form Approved

OMB No. 0704-0188

PLEASE DO NOT RETURN YOUR FORM TO THE ABOVE ADDRESS.

1. REPORT DATE *(DD-MM-YYYY)*	2. REPORT TYPE	3. DATES COVERED *(From - To)*
04-01-2001	Final	12 Jun 00 – 12 Dec 00

4. TITLE AND SUBTITLE

Tbit/s Optical Switches and Logic Gates: Towards Tunable Operation near 1.55 micro-meter

5a. CONTRACT NUMBER

F6256200M9154

5b. GRANT NUMBER

5c. PROGRAM ELEMENT NUMBER

6. AUTHOR(S)

Dr. Irina Talanina

5d. PROJECT NUMBER

5e. TASK NUMBER

5f. WORK UNIT NUMBER

7. PERFORMING ORGANIZATION NAME(S) AND ADDRESS(ES)

The Australian National University

Canberra 0200
Australia

8. PERFORMING ORGANIZATION REPORT NUMBER

N/A

9. SPONSORING/MONITORING AGENCY NAME(S) AND ADDRESS(ES)

AOARD
UNIT 45002
APO AP 96337-5002

10. SPONSOR/MONITOR'S ACRONYM(S)

AOARD

11. SPONSOR/MONITOR'S REPORT NUMBER(S)

AOARD-00-07

12. DISTRIBUTUION/AVAILABILITY STATEMENT

Approved for public release; distribution is unlimited.

13 SUPPLEMENTARY NOTES

14. ABSTRACT

In the performed research work, wavelength dependence (effects of detuning) and a possibility of tunable operation of the resonant soliton switches and logic gates have been investigated. A dramatic difference in the response of detuning between the semiconductor NLDC and atomic SIT-soliton NLDC has been revealed. A typical tunability range of a model resonant soliton NLDC has been assessed quantitatively and compared with a requirement for the device operating spectral range in WDM systems (applied by the gain bandwidth of erbium-doped fiber amplifiers). Extensive literature search has been performed to identify semiconductor materials which are suitable for implementation of the resonant soliton switches capable of tunable operation near the optical communication wavelength (1.55 micro-meters). A number of semi-conductor systems with the required excitonic absorption features have been selected including InGaAs/InAlAs MQW, InGaNAs/GaAs MQW, InGaAs/InP MQW, InGaAsP/InP MQW and GaSb/AlGaSb MQW structures. Modeling of operation of InGaAs/InAlAs MQW NLDC near 1.55 micro-meters has been performed; a tunability range of about 25 nm and a mean switching contrast ratio of 20:1 within this range have been demonstrated numerically. A new device design has been suggested as a possible way to substantially increase the device tunability range. In the new design, semiconductor quantum-dot-doped glass has been used as a material for the constituent waveguides of NLDC. The use of PbS quantum dots has lead to a broader device tunability range (at least, 65 nm) near 1.55 micro-meters.

15. SUBJECT TERMS

Non-linear Optics

16. SECURITY CLASSIFICATION OF:			17. LIMITATION OF ABSTRACT	NUMBER OF PAGES	19a. NAME OF RESPONSIBLE PERSON
a. REPORT	b. ABSTRACT	c. THIS PAGE			Michele Gaudreault, Maj, USAF
U	U	U	UU	22	19b. TELEPHONE NUMBER *(Include area code)* +81-3-5410-4409

Submitted to: Dr. Mark Nowack, AOARD, AFOSR
Dr. Arje Nachman, AFOSR/NM

Final Technical Report: F62562-00M9154

Tbit/s optical switches and logic gates: Towards tunable operation near 1.55 μm

Irina Talanina

Department of Theoretical Physics
Research School of Physical Sciences and Engineering
Australian National University
Canberra ACT 0200, Australia

Email: talanina@rsc.anu.edu.au

Performance Period: 1 July, 2000 – 31 December, 2000

Content

Research program performed during 1 July, 2000 – 31 December, 2000

Research program performed during 1 July, 2000 – 31 December, 2000

1. Outline of the completed tasks

Ultra-high-speed advanced optical processing technologies will lay a foundation for the direct support of future Tbit/s optical communication networks. In our recent work, a new scheme to implement Tbit/s optical switches and logic gates using a semiconductor nonlinear directional coupler (NLDC) has been proposed: a resonant soliton scheme [1,2]. Potential applications of this new class of devices in time division multiplexing (TDM) packet networks have also been investigated [3]. The aim of the present research program is to assess a feasibility of wavelength division multiplexing (WDM) applications of the resonant soliton switches.

In the performed numerical work, wavelength dependence (effects of detuning) and a possibility of tunable operation of the resonant soliton switches and logic gates have been investigated. A dramatic difference in the response to detuning between the semiconductor NLDC and atomic SIT-soliton NLDC has been revealed. A typical tunability range of a model resonant soliton NLDC has been assessed quantitatively and compared with a requirement for the device operating spectral range in WDM systems (applied by the gain bandwidth of erbium-doped fiber amplifiers). Extensive literature search has been performed to identify semiconductor materials which are suitable for implementation of the resonant soliton switches capable of tunable operation near the optical communication wavelength (1.55 μm). A number of semiconductor systems with the required excitonic absorption features have been selected including InGaAs/InAlAs MQW, InGaNAs/GaAs MQW, InGaAs/InP MQW, InGaAsP/InP MQW and GaSb/AlGaSb MQW structures. Modeling of operation of InGaAs/InAlAs MQW NLDC near 1.55 μm has been performed; a tunability range of about 25 nm and a mean switching contrast ratio of 20:1 within this range have been demonstrated numerically. A new device design has been suggested as a possible way to substantially increase the device tunability range. In the new design, semiconductor quantum-dot-doped glass has been used as a material for the constituent waveguides of NLDC. The use of PbS quantum dots has lead to a broader device tunability range (at least, 65 nm) near 1.55 μm.

2. Overview of recent advances in WDM transmission systems

During the last decade, long-distance optical transmission systems have advanced from the transmission rates of 140 Mbit/s to transathlantic lines with the rates in access of 1 Tbit/s. In these ultra-high-speed communication systems, Tbit/s aggregate capacity is achieved by combining many WDM channels, each with a distinct wavelength, with ultra-high-bit-rate optical TDM signals transmitted in each channel. Laboratory demonstrations of optical transmission at 100 Gbit/s per channel and use of over 132 channels in a single fiber are currently in progress.

In current WDM systems, the transmission capacity is limited by the gain bandwidth of erbium-doped fiber amplifiers (EDFAs). A conventional EDFA has a gain bandwidth of about 35 nm (~4.4 THz, see Fig. 1). This allows, for example, a WDM transmission with 1 Tbit/s aggregate capacity in the wavelength span of 1532-1562 nm by employing 25 different wavelength channels and a line rate of 40 Gbit/s per channel [4]. A gain-shifted EDFA supports WDM signals in the longer wavelength region of 1570-1600 nm [5]. The WDM transmission capacity can be increased by developing EDFAs with a broader gain bandwidth, by employing

a higher line rates, and by improving the spectral efficiency of WDM signals. For example, a newly developed gain-flattened tellurite-based EDFA has a gain bandwidth of about 80 nm [6]. Employing this broad bandwidth amplifier, 3 Tbit/s aggregate capacity transmission with 19 WDM channels of 160 Gbit/s OTDM signals has been recently reported [7]. The wavelength of the 19 channels ranged from 1540 to 1609 nm with a channel spacing of 480 GHz.

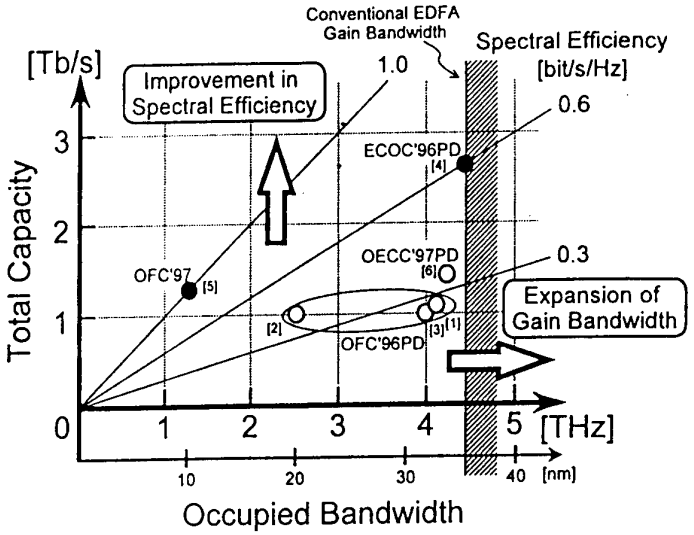

FIG. 1. Recent advances in Tbit/s optical transmission experiments [Ref. 8].

These latest developments, in combination with rapid growth in data and Internet traffic, have lead to a strong demand for new technologies to support ultra-high-speed optical transmission systems. The lack of advanced optical switching/logic technologies and the use of electronic devices instead results in severe performance bottleneck in ultra-high-speed backbone networks. Therefore, new concepts in implementation of Tbit/s low-latency all-optical switches and logic gates are presently of great interest.

In our recent work, a novel scheme to achieve Tbit/s optical switching and logic functions in a semiconductor NLDC has been proposed: a resonant soliton scheme [1,2]. Potential applications of the resonant soliton devices for optical packet processing in TDM networks have been investigated [3]. Main focus of the present project has been to explore a possibility of WDM applications of the resonant soliton switches. This has involved a general investigation of the possibility of tunable operation of the resonant soliton NLDC as well as an identification of semiconductor materials which are suitable for implementation of the resonant soliton devices with an operating wavelength near 1550 nm. An operating wavelength of the resonant soliton switches and logic gates is determined by an optical bandgap of the corresponding semiconductor MQW structure and, in particular, by a spectral position of the $1s$-exciton resonance near the bandedge [1]. There are a number of semiconductor materials which have excitonic resonances in the spectral range near the optical communication wavelength (see Sec. 4, Task 2). For TDM applications, where optical data are transmitted in a single wavelength channel, the question of tunability of the resonant soliton devices does not arise. In contrast, potential WDM applications depend crucially on whether the device permits tunable operation in the spectral window employed in WDM communications.

A primary focus of the present numerical investigation has been to assess whether the resonant soliton switches allow tunable operation, and if so, whether their tunability range can match the gain bandwidth of the conventional EDFA, *i.e.* about 35 nm. A further focus has been to explore possible ways to extend the tunability range. To address these issues, a general investigation of wavelength dependence of a resonant soliton switch has been performed first (see Task 1). It has been followed by an extensive search and analysis of various semiconductor materials potentially suitable for implementation of the tunable resonant soliton switches for WDM applications (see Task 2). Numerical simulations and assessment of the device operation near 1550 nm have been performed with the material parameters of one of the semiconductors identified in Task 2 (see Task 3). A possible new approach to achieving a much broader tunability range for the resonant soliton devices has also been discussed (see Task 4).

3. Numerical Method

A basic numerical code describing the operation of a semiconductor NLDC in the resonant excitation regime has been developed in our recent work [1]. This code applies to a directional coupler with two-arm branches (2×2 NLDC). In the performed program, the code has been extended to allow for a variable detuning from the $1s$-exciton resonance. The mathematical formalism is briefly described below.

Based on a coupled-mode approach, the reduced Maxwell-semiconductor Bloch equations (MSBE) are solved for single-mode waveguides in the case of near resonant excitation at the $1s$-exciton resonance:

$$\frac{\partial E_j(\xi,\eta)}{\partial \xi} = i\frac{2\pi}{c^2}\frac{\omega_L^2}{k_L}P_j(\xi,\eta) + iKE_l(\xi,\eta), \tag{1}$$

$$\frac{\partial P_j(\xi,\eta)}{\partial \eta} = -i\left[\delta + \beta_1|P_j(\xi,\eta)|^2 - i\gamma_2\right]P_j(\xi,\eta) + \frac{id_{cv}}{2\hbar}\left[1 - \beta_2|P_j(\xi,\eta)|^2\right]E_j(\xi,\eta), \tag{2}$$

where $E(\xi,\eta)$ and $P(\xi,\eta)$ are complex amplitudes of the electric field and the induced polarization in the moving coordinate frame ($\xi = z$ is a propagation coordinate, $\eta = t - z/U$ is a time coordinate, U is a group velocity of the pulse), $j,l = 1,2$ ($j \neq l$), $\delta = \omega_{1s} - \omega$ is a detuning of the input field frequency from the $1s$-exciton resonance, β_1 and β_2 are nonlinear exchange and phase-space filling parameters, γ_2 is a phenomenological dephasing rate, and K is a coupling coefficient. The model assumes a large exciton binding energy (E_b), thus allowing higher exciton and continuum states to be neglected. For femtosecond light pulses with moderate intensities, the neglect of screening is justified.

Eqs.(1)–(2) have been solved using the fourth-order Runge-Kutta method which has been described in our previous studies [1,9]. An input has been given by a sech-shaped pulse $E(\xi = 0,\eta) = E_0\mathrm{sech}(\eta/\tau)$ with a 100-fs duration (FWHM). The switching behaviour of the pulse has been monitored by computing the pulse intensity profile, the pulse energy, and the pulse area transmitted through each channel. To assess high-repetition operating characteristics of the NLDC, various sequences of the input pulses have been launched in channel 1. Unless specified otherwise, the time delay between the pulses has been set to 500 fs which corresponds to the switch throughput of 2 Tbit/s.

The numerical simulations have been performed using the existing computer facilities of the Theoretical Physics Department, RSPhysSE, Australian National University: Unix DEC Alpha Workstations with the operating speed up to 500 MHz.

4. Tunable operation of Tbit/s optical switches near 1.55 μm

Task 1. Wavelength dependence of a resonant soliton NLDC

The main objective in this Task is to perform a general investigation of wavelength dependence of the resonant soliton NLDC. In our previous studies, a carrier wavelength of the incident optical pulse has been tuned exactly at the $1s$-exciton resonance [1,2], and the effects of detuning have not been of interest in the context of potential TDM applications [3]. In this project, a possibility of tunable operation of the resonant soliton NLDC is a key issue directly related to potential applications in WDM systems. To allow direct comparison with the results of our previous studies, the material parameters of II-VI semiconductor (CdZnTe/ZnTe MQW) structures [12] have been chosen in the simulations of this Task. This material system is characterized by a large value of the exciton binding energy (23 meV) which is essential to achieve high device performance.

An operation of 2×2 NLDC in the regime of off-resonance excitation ($\delta \neq 0$) has been modeled. The excitonic resonance has been assumed to be homogeneously broadened, and the sharp line approximation has been applied. The detuning has been measured in the units of meV to allow direct comparison with the exciton binding energy. Note that the spectral width of the incident 100-fs pulse is smaller than the exciton binding energy, however, it is much larger than the exciton linewidth.

When the input pulse is detuned from the $1s$-exciton resonance, an extra term proportional to the detuning affects the real part of the polarization in Eq. (2) in comparison with the case of on-resonance excitation. In particular, the polarization field originating from the exciton-exciton interaction [β_1-term in Eq. (2)] is directly influenced by the detuning.

Shown in Fig. 2 are numerical results on the NLDC operation in the case of negative and positive detunings (excitation above and below the resonance, respectively). When the detuning is small, for example, $|\delta| = 2$ meV, there is only a minor change in the switch operation in comparison with the case of on-resonance excitation (see two top graphs in Fig. 2). Depending on the sign of δ, the curves shift slightly towards higher or lower cross-over switching pulse area. Note that, in the case $\delta = 0$, the cross-over pulse area for switching is 0.75π. In the case of moderate detuning, for example, $|\delta| = 5$ meV, the changes in the switch operation become more pronounced and strongly depend on the sign of δ. At the negative detuning (left middle graph in Fig. 2), the main change is that the curves are strongly shifted towards larger pulse areas. At the positive detuning (right middle graph in Fig. 2), the curves are strongly shifted towards smaller pulse areas. A striking difference between the switching behaviour at negative and positive detunings is that, in the latter case, the curves do not cross. In the case of strong detuning, for example, $|\delta| = 10$ meV, the changes in the switch operation become quite dramatic and again strongly depend on the sign of δ. At the negative detuning (left bottom graph in Fig. 2), a further strong shift towards larger pulse areas is observed together with a strong restructuring of the shifted curves. In contrast, at the positive detuning (right bottom graph in Fig. 2), the switch response becomes essentially independent of the input pulse area.

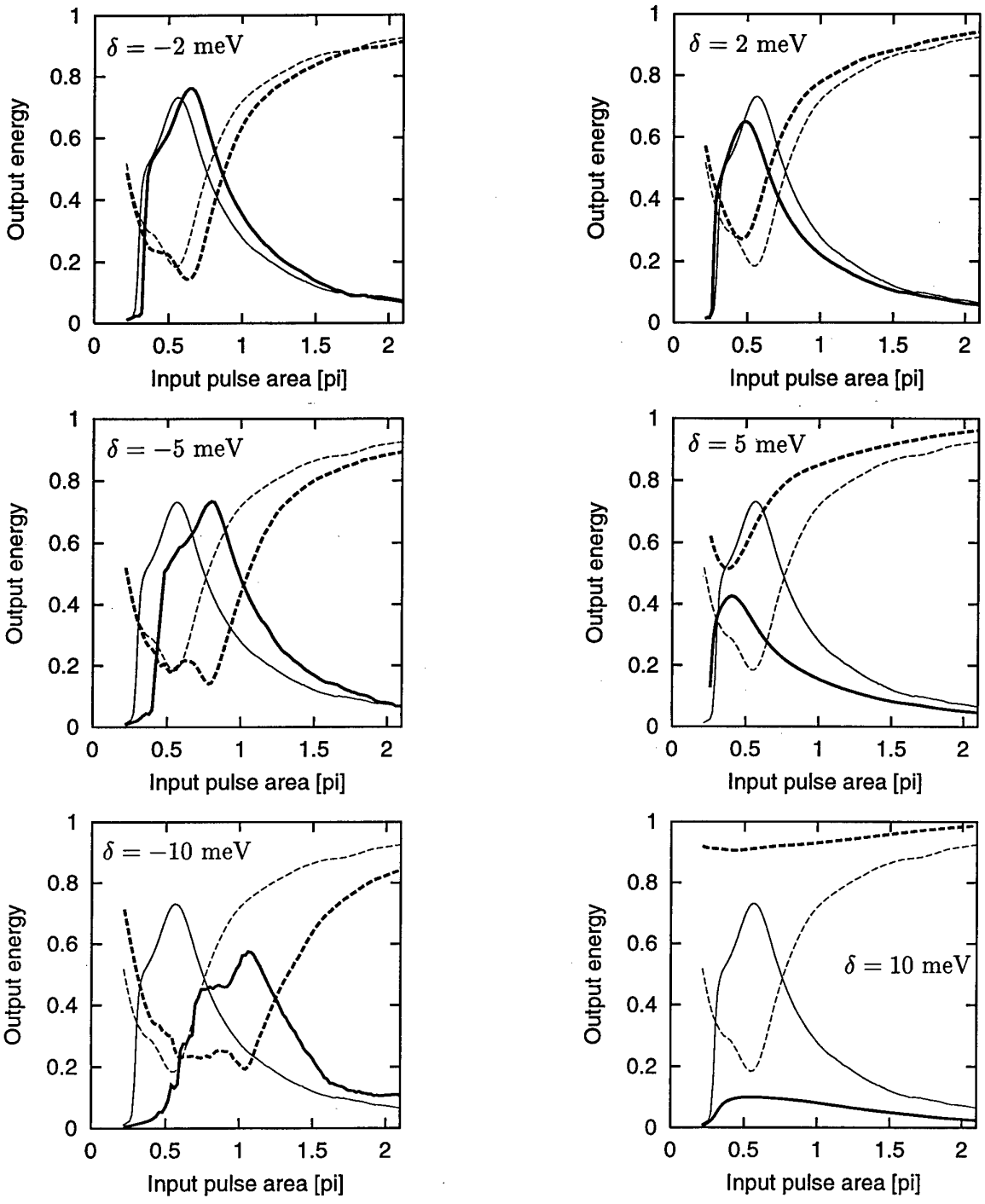

FIG. 2. Output energy (normalized to the input energy) vs. input pulse area for six different values of detuning of the pulse carrier frequency from the 1s-exciton resonance ($z = L_c$). An input 100-fs pulse is launched in channel 1 of the NLDC. Thick solid line shows an output of the NLDC in channel 1, and thick dashed line shows an output of the NLDC in channel 2. For comparison, thing solid and dashed lines show outputs in channels 1 and 2, respectively, in the case of on-resonance excitation ($\delta = 0$). The switch response in the case of negative detunings (excitation above the resonance) and positive detunings (excitation below the resonance) is compared (see left and right columns, respectively).

The results presented in Fig. 2 demonstrate that an increase in the detuning causes a very strong change in the NLDC response in the regime of small-to-medium input pulse areas (0.5π – 1.3π). **A surprising result is that the switch operation in the regime of strong input pulses (the pulse area larger than 1.5π) is almost unaffected by the detuning.** This result is unexpected because it is opposite to what happens in the case of atomic systems [10]. In the case of an atomic SIT-soliton switch, only for small values of the detuning the operation of the switch still persists (see Fig. 6c in Ref. [10]), whereas large detunings completely destroy the switch operation, even for strong input pulses (see, for example, Fig. 6a in Ref. [10]).

To understand physical reasons for such a drastic difference in operation of the excitonic switch and the atomic SIT-soliton switch in the case of large detunings, one needs to compare the mechanisms of the nonlinearity in both these cases. In the excitonic polarization equation (2), there are two nonlinear terms: β_1 exchange term and β_2 phase-space filling term (see Sec. 3 above). Only the phase-space filling term has a direct analog in the atomic systems, where, in fact, this term is responsible for the SIT-soliton switching mechanism, as shown in Ref. [10]. In the excitonic case, however, the β_1 exchange term which results from the exciton-exciton interactions has been shown to be a dominant nonlinear term in the excitonic polarization equation in the case of bulk semiconductors [9]. This term has no analogy in the atomic polarization equation (an analog would be atom-atom interactions which are negligible) [10]. An increase in detuning from the resonance drastically affects the phase-space filling process, however, it appears to produce only a minor change in the exciton-exciton interactions which remain relatively strong even for quite large values of the detuning (*i.e.*, comparable with the exciton binding energy). For example, the exciton-exciton interactions in the off-resonance case have been shown to lead to a formation of so-called polariton solitons (though the corresponding soliton solution has been derived solving a different set of equations) [11].

On the basis of the numerical results presented in Fig. 2, one can conclude that, a reason for the switch operation in the regime of strong input pulses being almost unaffected by the detuning is the fact that, in this regime, the magnitude of the β_1 exchange term in Eq. (2) remains much larger than the magnitude of the δ-related term for any reasonable values of δ (note that the detunings are limited to the spectral region where the excitonic MSBE remain valid.

The numerical results obtained in the regime of strong input pulses and large detunings demonstrate that, in contrast to the atomic SIT-soliton switch which only operates in a very narrow spectral region defined by the atomic resonant transition, the excitonic switch maintains effective operation even in the case when the input field is strongly detuned from the $1s$-exciton resonance. The device performance, however, is substantially higher in the case of positive detunings (below the resonance) than in the case of negative detunings (above the resonance). For example, Fig. 3 illustrates the switch response in the case of high-repetition operation under strong negative and positive detunings. The input is given by a train of four 100-fs pulses, each with pulse area of 1.5π, launched in channel 1 and separated in time by 500 fs (see Fig. 3a). The switch throughput is 2 Tbit/s. An efficient NLDC operation takes place in the case of the positive detunings (see Fig. 3d,e) as well as in the case $\delta = 0$ which is shown for comparison (see Fig. 3c), however, in the case of the negative detuning, the device performance degrades substantially (see Fig. 3b). It is therefore preferable to operate in the spectral region below the resonance rather than above. Note that, with an increase in the detuning below the resonance, a progressive pulse narrowing occurs, however, no signs of pulse break-up appear.

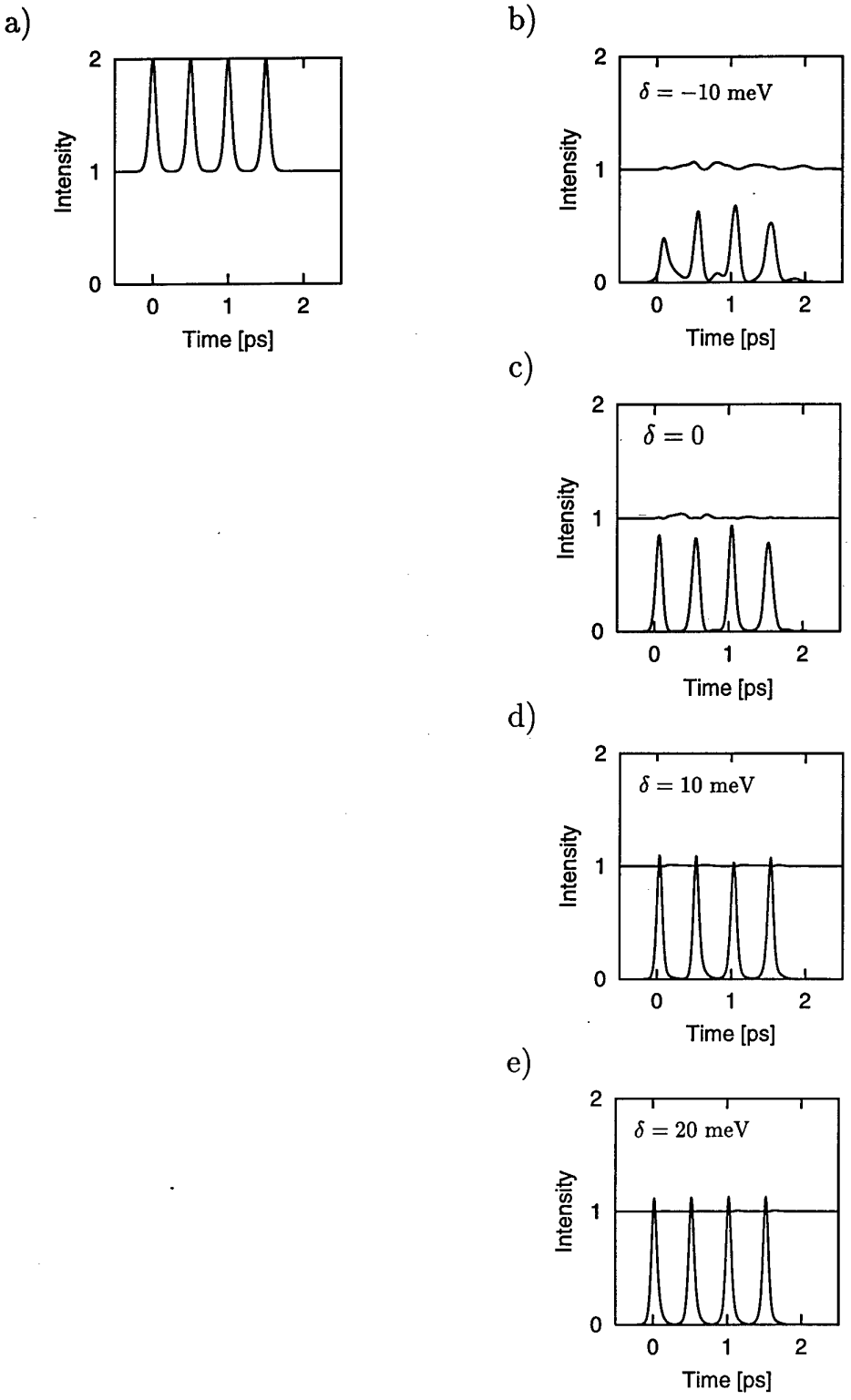

FIG. 3. An operation of the resonant soliton NLDC in high-repetition regime under various detunings from the $1s$-exciton resonance ($z = L_c$). The input is given by a train of four 100-fs pulses, each with a pulse area of 1.5π, launched in channel 1 and separated in time by 500 fs (a). Temporal profiles of the transmitted pulses are shown for four different values of the detuning: (b) $\delta = -10$ meV; (c) $\delta = 0$; (d) $\delta = 10$ meV; (e) $\delta = 20$ meV.

A key issue in relation to the device tunability and potential WDM applications is to assess quantitatively whether it is feasible to meet the specific tunability requirement applied by a gain bandwidth of conventional EDFAs in WDM transmission networks. As discussed in Sec. 2 above, this bandwidth is about 35 nm allowing WDM transmission in the wavelength span of, for example, 1532-1562 nm (in eV units, this corresponds to 0.809 eV – 0.794 eV). Alternatively, a gain-shifted EDFA supports WDM signals in the longer wavelength region of 1570-1600 nm (in eV units; this corresponds to 0.790 eV – 0.775 eV). Thus, the WDM spectral window defined by the use of conventional EDFAs requires the device tunability range to be about 15 meV.

Plotted in Fig. 4 is a numerical dependence of the switching contrast ratio on detuning from the 1s-exciton resonance for the resonant soliton NLDC with CdZnTe/ZnTe MQWs material parameters. As seen from Fig. 4, the switching contrast ratio increases monotonically from a region of negative detunings towards positive detunings. A comparison between two plotted curves, corresponding to 2π input pulse and 1.5π input pulse, demonstrates that the switching contrast ratio is generally higher in the case of stronger pulses. The operating spectral range of the device is about 25 meV. This value is two times larger than the specific WDM requirement discussed above. Within this tunability range, the switching contrast ratio is, in average, very high (about 20:1), however, it changes quite rapidly throughout the range, overall by an order of magnitude. This dependence is determined by the ratio of the total energy transmitted through channel 2 to the total energy transmitted through channel 1. While the former value approaches 1, the latter goes to 0 (see Fig. 2) resulting in the rapid dependence shown in Fig. 4. In reality, any experimental detection system has a sensitivity limit due to which the corresponding measured dependence will reach a saturation level.

Based on the results obtained in this Task, one can conclude that the resonant soliton switches do allow tunable operation, and WDM applications of these novel devices are feasible. This conclusion equally applies to the resonant soliton logic gates as the underlying physics of their operation is the same [2].

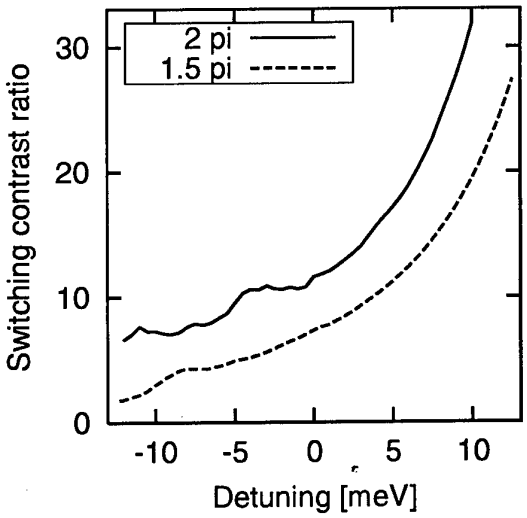

FIG. 4. Switching contrast ratio vs. detuning from the 1s-exciton resonance for CdZnTe/ZnTe MQW NLDC with two different input pulse areas: 2π (solid line) and 1.5π (dashed line).

Task 2. Semiconductor materials for device operation near 1.55 μm

An extensive literature search has been undertaken to identify semiconductor materials suitable for implementation of the tunable resonant soliton switches operating at wavelengths near 1.55 μm. A number of semiconductor MQW systems have been selected and are discussed below. It should be noted that suitable semiconductor materials are not limited to those listed below; the selection has been performed on the basis of availability of published data.

InGaAs/InAlAs

InGaAs/InAlAs MQW structures appear to be one of the most promising material systems for implementation of the resonant soliton devices. This is mostly due to their large optical nonlinearity at 1.55 μm associated with the excitonic features. Well-resolved heavy-hole (HH) and light-hole (LH) exciton resonances in the absorption spectra of these structures have been reported at temperatures as high as 460 K (see Fig. 5a) [13]. The spectral position of the $n = 1$ HH exciton peak shifts from $\sim$1.4 μm at 81 K to $\sim$1.6 μm at 460 K, and it is located near 1.5 μm at room temperature [14]. In eV units, the corresponding energy is $\sim$0.778 eV for HH exciton and $\sim$0.807 eV for LH exciton at about 300 K. The HH exciton binding energy in InGaAs/InAlAs MQWs has been estimated to be 6 meV [13]. Note that this is a much smaller value than those typical for II-VI semiconductors.

InGaAs/InAlAs MQW structures are usually grown by molecular beam epitaxy on InP substrate. Changing the width of InGaAs wells from about 40$\AA$ to about 130$\AA$, a large shift in the spectral position of the HH exciton (up to 150 nm) can be achieved [13,15]. This opens up a possibility to control the excitonic band position via a proper MQW design. Such a control is very important for device applications because it allows to optimize the device performance and to ensure that the device tunabily range covers the spectral region occupied by WDM channels. A substantial shift of the excitonic absorption peak can be also achieved in strained MQWs. For example, highly strained $In_{0.66}Ga_{0.34}As/In_{0.30}Al_{0.70}As$ MQW structures with no degradation in the excitonic features have been reported in Ref. [15]. As seen from Fig. 5b, the spectral position of the HH exciton has been shifted about 50 nm towards longer wavelengths from that of the lattice-matched InGaAs/InAlAs MQWs at room temperature [15].

It should be added that, using Be-doped strained InGaAs/InAlAs MQWs, Tbit/s demultiplexing and all-optical AND gate operating at 1.55 μm have been recently reported [16]. These devices have utilized carrier induced saturable excitonic absorption in a surface reflection geometry. A compressive strain has been applied to the quantum wells in order to enhance the excitonic optical nonlinearity [17]. While the reflection geometry is conceptually different from the approach adopted in our work, the corresponding experiments have clearly demonstrated a great potential of InGaAs/InAlAs MQW structures as a prime candidate for implementation of ultrafast excitonic devices.

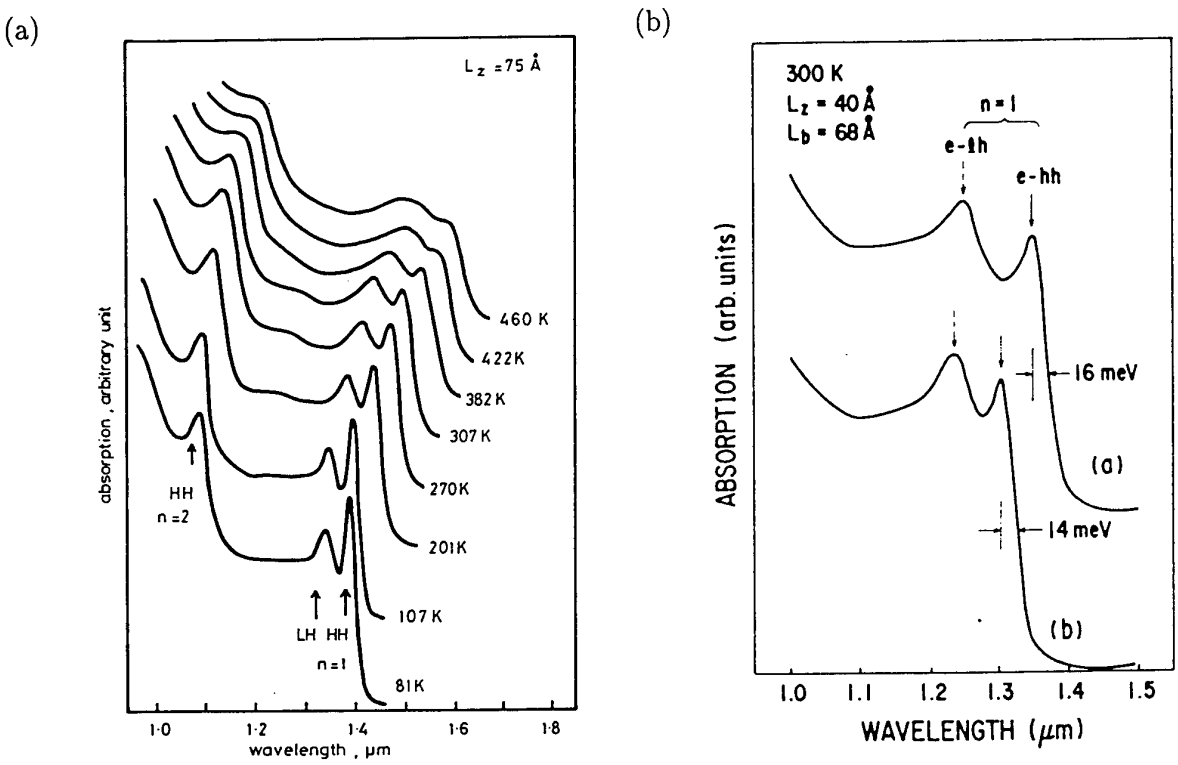

FIG. 5. (a) Optical absorption spectra of InGaAs/InAlAs MQW structures: (a) at different temperatures (the experimental results are taken from Ref. [13]); (b) for highly strained structures (upper curve) and lattice-matched structures (lower curve) [15].

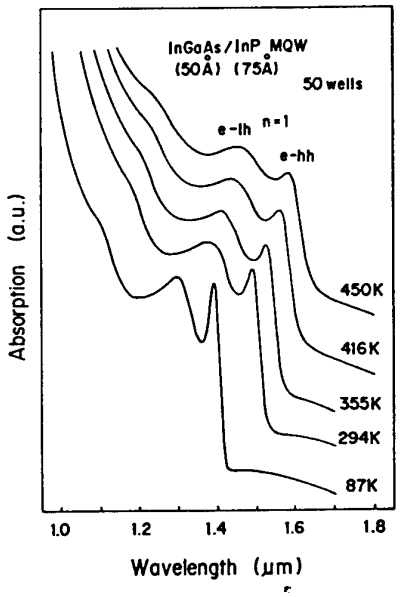

FIG. 6. Optical absorption spectra of InGaAs/InP MQW structures (the experimental results are taken from Ref. [18]).

InGaAs/InP

Another candidate for WDM applications near 1.55 μm is InGaAs/InP MQW structures. These structures are also lattice matched to InP and can be grown using various techniques including metallorganic molecular beam epitaxy [18]. HH and LL excitonic resonances in the absorption spectra of InGaAs/InP MQW have been reported at temperatures up to 450 K (see Fig. 6) [18]. The spectral position of the HH exciton peak at room temperature is near 1.5 μm, and it can be adjusted by changing the InGaAs well thickness in a wide range (typically, from 10$\AA$ to 2000$\AA$). In general, the excitonic features in InGaAs/InP MQW and InGaAs/InAlAs MQW structures are quite similar, however, the latter ones have an advantage due to their large conduction band discontinuity (0.5 eV) comparing with that (0.2 eV) of the former ones.

InGaNAs/GaAs

New promising material systems incorporating nitrogen have been recently discovered. This includes InGaNAs which was proposed and created in 1995 [19]. New InGaNAs/GaAs structures have been presented as an alternative to InP-based materials for implementation of long-wavelength-range laser diodes (1.3–1.55 μm range) [19,20]. A replacement of only a few percent of the arsenic atoms by nitrogen reduces the band gap in InGaNAs in comparison with InGaAs by up to several hundred meV. Due to this red shift, the photoluminescence (PL) wavelength of InGaNAs lies near the technologically important 1.3–1.55 μm range (see Fig. 7a) [19]. The PL wavelength could be elongated by increasing the amount of nitrogen and indium [21]. It should be added that the new InGaNAs structures also exhibit drastically improved high-temperature performance characteristics (in comparison with InP-based materials) [19,20].

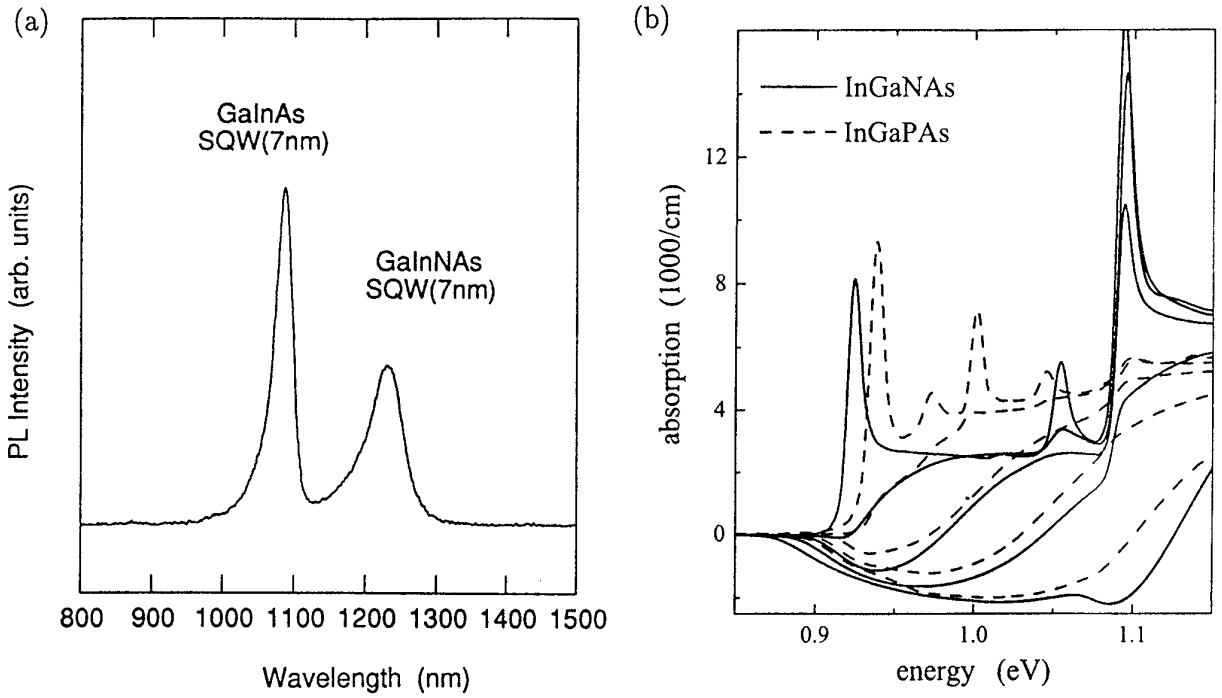

FIG. 7. (a) Photoluminescence spectra of InGaNAs and InGaAs at room temperature (the experimental results are taken from Ref. [19]). (b) Optical absorption and gain spectra for a 6 nm $In_{0.3}Ga_{0.7}N_{0.02}As_{0.98}$ QW between 10 nm GaAs barriers (solid lines) and a 6 nm $In_{0.67}Ga_{0.33}P_{0.28}As_{0.72}$ QW between InP barriers (dashed lines) for carrier density (from top to bottom) of 0.25, 1.0, 2.5, 5.0 and 10×10^{12} cm^{-2} (the numerical results are taken from Ref. [22]).

The excitonic features in InGaNAs/GaAs structures have not yet received much attention in experimental investigations (no reports on the excitonic effects in InGaNAs have been found in experimental literature so far). However, the absorption spectra of InGaNAs/GaAs structures at different carrier densities have been recently calculated [22]. Shown in Fig. 7b are the absorption and gain spectra for a 6 nm $In_{0.3}Ga_{0.7}N_{0.02}As_{0.98}$ well and a 6 nm $In_{0.67}Ga_{0.33}P_{0.28}As_{0.72}$ well for carrier density in the range 0.25–10 $\times 10^{12}$ cm^{-2} [22]. A strong excitonic absorption peak ($n = 1$ HH-exciton) is clearly seen at 922 meV at low carrier densities (the corresponding wavelength is 1.35 μm).

At present, due to the lack of experimental data on excitonic effects in InGaNAs/GaAs structures, it is difficult to draw any final conclusions on suitability of this material system for implementation of the resonant soliton switches. However, if an experimental absorption spectrum would show the same or very close excitonic features as those in the calculated spectrum of Fig. 7b [22], than InGaNAs/GaAs structures would possibly be rated as the best material system for implementation of the resonant soliton devices.

InGaAsP/InP

Another possible candidate for implementation of the resonant soliton switches is InGaAsP/InP MQW structures. Their fundamental absorption features have been reported for different alloy compositions, for example, $In_{0.73}Ga_{0.27}As_{0.6}P_{0.4}$ with the bandgap wavelength of 1.3 μm [23]. A refractive index for the above composition at 1.5 μm is 3.35. The excitonic absorption peaks can be clearly seen from the calculated absorption spectra (see Fig. 7b [22]). InGaAsP/InP MQW structures appear to be generally suitable for implementation of the resonant soliton devices.

GaSb/AlGaSb

This semiconductor material system may be of interest for device operation at slightly longer wavelengths than 1.55 μm. GaSb/AlGaSb MQW structures have not attracted much attention in the literature (in comparison with GaAs-based and InP-based materials), however, their excitonic features have been studied. A clear double-peak structure in the excitonic absorption band has been observed in GaSb(7 nm)-$Al_{0.25}Ga_{0.75}Sb$(3 nm) MQWs at temperatures ranging from 81 to 300 K (see Fig. 8) [24]. The double-peak is associated with the $n = 1$ heavy and light hole excitons (the longer and shorter wavelength, respectively), with the HH exciton spectral position at about 1.6 μm. This material system might be of interest for device applications in the longer wavelength region (1570-1600 nm) associated with the gain-shifted EDFAs in WDM systems [5] as mentioned in Sec. 2 above.

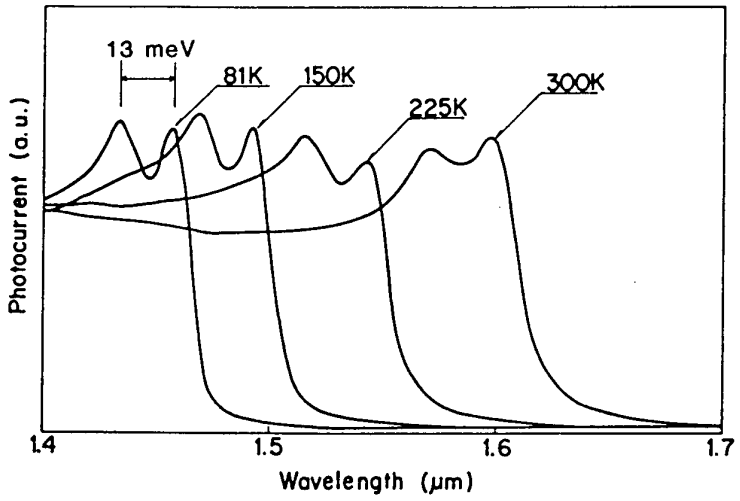

FIG. 8. Photocurrent spectra of GaSb/AlGaSb MQW structures at temperatures ranging from 81 to 300 K (the experimental results are taken from Ref. [24]). The double-peak is associated with $n = 1$ HH and LH excitons (the longer and shorter wavelength, respectively).

Task 3. Operation of InGaAs/InAlAs MQW NLDC

InGaAs/InAlAs MQW material parameters have been chosen in the simulations of the device operation near the optical communications wavelength because of the presence of quite extensive data in the literature on this material system and, in particular, on the corresponding excitonic parameters [13–17]. It should be emphasized that qualitative features of the resonant soliton NLDC operation do not depend on a choice of semiconductor material parameters, however, quantitative differences in the device operating characteristics do exist.

Due to the fact that the exciton binding energy in InGaAs/InAlAs MQW structures (about 6 meV) is a few times smaller than the corresponding value in CdZnTe/ZnTe MQW systems, a duration of the input pulses in the simulations of this Task has been chosen to be 200 fs (instead of 100 fs in Task 2 above) to reduce the spectral width of the pulse. The excessive spectral width leads to increased excitation of continuum states and enhanced polarization dephasing rates which result in degradation of the device performance. A time delay between the consecutive input pulses has been set to 1 ps corresponding to the device throughput of 1 Tbit/s.

Shown in Fig. 9 are numerical results on InGaAs/InAlAs MQW NLDC operation in the case of negative and positive detunings (the excitation above and below $n = 1$ HH exciton resonance, respectively). Note that, for the well width of 75 $\AA$, a spectral position of the resonance is at $\sim$1500 nm (at room temperature), according to the experimental data of Ref. [13]. A dependence of the output energy on the input pulse area is plotted in Fig. 9 for four different values of detuning from the resonance. When the detuning is relatively small and above the resonance, there is only a minor change in the switch operation in comparison with the case of on-resonance excitation (see top left graph in Fig. 9). The curves merely shift towards higher input pulse areas. Note that, in the case $\delta = 0$, a cross-over pulse area for switching is 0.85π

which is slightly higher than for CdZnTe/ZnTe system (see Task 1 above). For the same value of the detuning below the resonance, a change in the switch operation becomes more pronounced, in particular, the curves do not cross any more (see top right graph in Fig. 9).

In the case of strong detunings (comparable with E_b), the changes in the output/input dependence become quite dramatic and strongly depend on the sign of δ. At the negative detuning (bottom left graph in Fig. 9), the main change is that the curves are strongly shifted towards larger pulse areas and show strong restructuring. At the positive detuning (bottom right graph in Fig. 9), the switch response becomes almost insensitive to the input pulse area. While the general behaviour of InGaAs/InAlAs MQW NLDC is qualitatively similar to that of CdZnTe/ZnTe MQW NLDC discussed in Task 1 above, the tunability range of the device is substantially reduced. This is attributed to the small value of the exciton binding energy in this system.

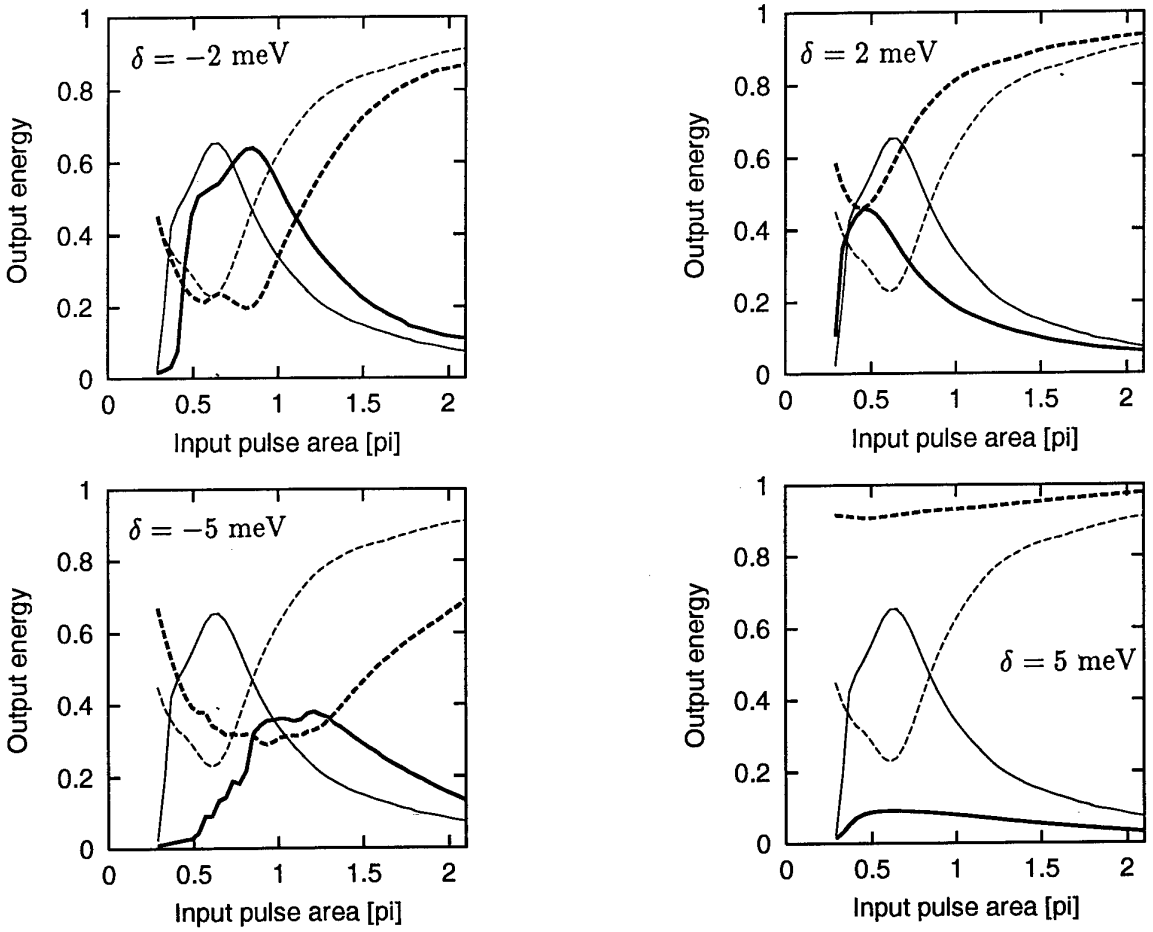

FIG. 9. Output energy (normalized to the input energy) vs. input pulse area for four different values of detuning of the pulse carrier frequency from the 1s-exciton resonance in InGaAs/InAlAs MQW NLDC ($z = L_c$). An input 200-fs pulse is launched in channel 1 of the NLDC. Thick solid line shows an output of the NLDC in channel 1, and thick dashed line shows an output of the NLDC in channel 2. For comparison, thing solid and dashed lines show output in channels 1 and 2, respectively, in the case of on-resonance excitation ($\delta = 0$). The switch response in the case of negative detunings (excitation above the resonance) and positive detunings (excitation below the resonance) is compared (see left and right columns, respectively).

Fig. 10 illustrates the switch response in the case of high-repetition operation under the strong negative and positive detunings. The input is given by a train of four 200-fs pulses, each with pulse area of 2π, launched in channel 1 and separated in time by 1 ps (see Fig. 10a). Efficient NLDC operation with a throughput of 1 Tbit/s takes place in the case of positive detunings (see Fig. 10d) as well as in the case $\delta = 0$ (see Fig. 10c), however, in the case of negative detuning, the device performance degrades substantially (see Fig. 10b). Therefore, similar to the conclusion made in Task 1 above, it is preferable to operate in the spectral region below the resonance rather than above to enhance the device performance. A comparison between Figs. 4 and 10 also illustrates the reduced tunability range of InGaAs/InAlAs MQW NLDC.

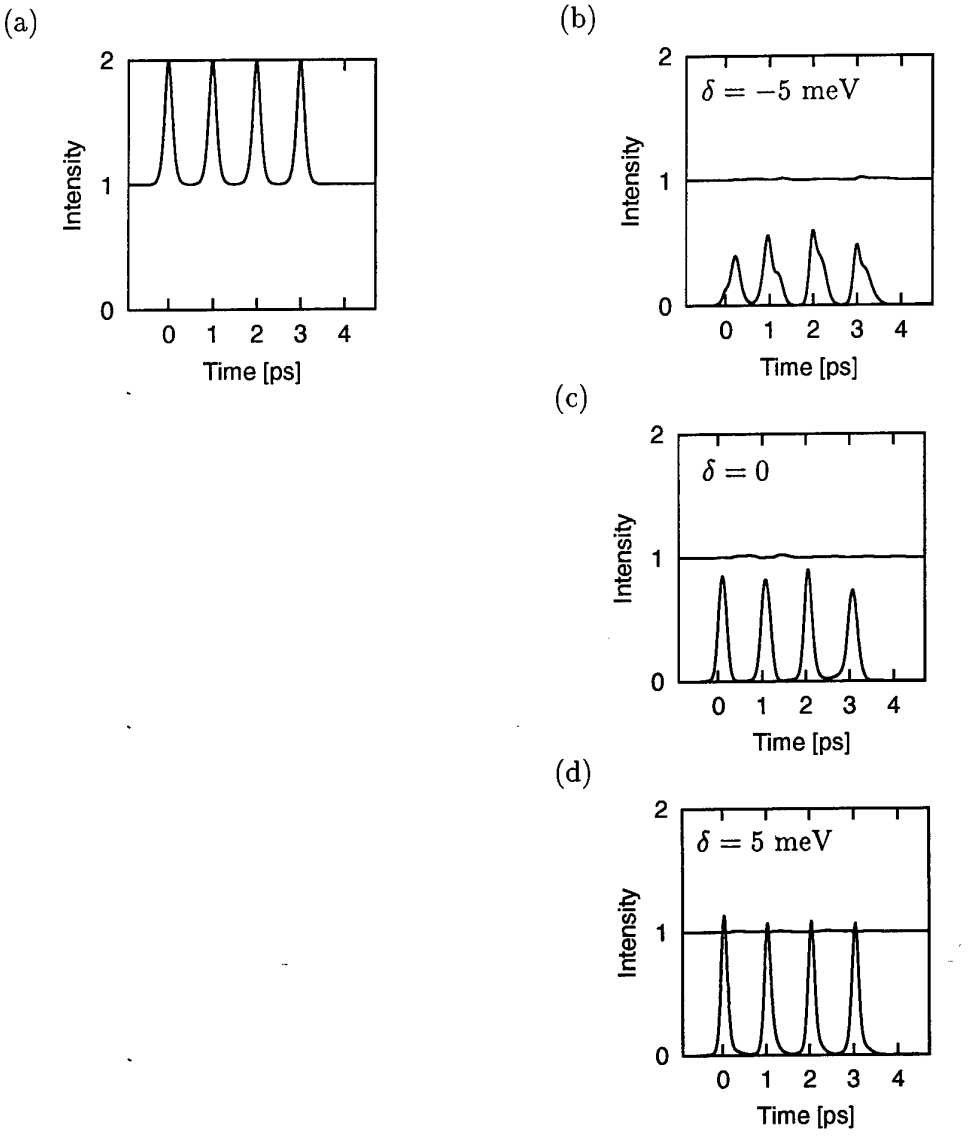

FIG. 10. The operation of InGaAs/InAlAs MQW NLDC in high-repetition regime under large detunings from the exciton resonance ($z = L_c$). The input is given by a train of four 200-fs pulses, each with a pulse area of 2π, launched in channel 1 and separated in time by 1 ps (a). Temporal profiles of the transmitted pulses are shown for three different values of the detuning: (b) $\delta = -5$ meV; (c) $\delta = 0$; (d) $\delta = 5$ meV.

Plotted in Fig. 11 is a numerical dependence of the switching contrast ratio on detuning from the exciton resonance. The switching contrast ratio increases monotonically from a region of negative detunings towards positive detunings. A comparison between two plotted curves, corresponding to 2π and 1.5π input pulses, demonstrates that the switching contrast ratio is generally higher in the case of stronger pulses. The tunability range of the device extends roughly from $\delta = -4$ meV to $\delta = 8$ meV, leading to a spectral operating window of about 12 meV (about 25 nm). This is comparable with the target value of 15 meV discussed in Task 1. Taking into account that a moderate increase in the tunability range (up to 20%) can be achieved via routine device optimization, it is therefore expected that the resonant soliton devices fabricated on optimized InGaAs/InAlAs MQW structures will be able meet the specific tunability requirement applied by the use of the conventional EDFAs in WDM transmission systems.

Some conclusions can be made about the prospects for the resonant soliton switches to match the 80-nm gain bandwidth of the tellurite-based EDFA. InGaAs/InAlAs MQW NLDC does not show a potential to meet this particular requirement which is equivalent to tripling the tunability range of the device. A straightforward solution to the problem would be to exploit a semiconductor MQW system characterized by an extremely large value of the exciton binding energy (such as, for example, several tens of meV). Such large values of E_b are known for some bulk semiconductors (for example, CuCl), but not for III-V semiconductor MQW systems of practical interest. Thus, further advances and/or new developments in semiconductor material systems are necessary to meet the 80-nm goal. On the other hand, an alternative approach based on a different device design might be exploited. Namely, a semiconductor quantum-dot-doped glass can be used as a material for the constituent waveguides of the NLDC. This approach, though technologically challenging and conceptually complex, is worthwhile to investigate, and it is discussed in Task 4 below.

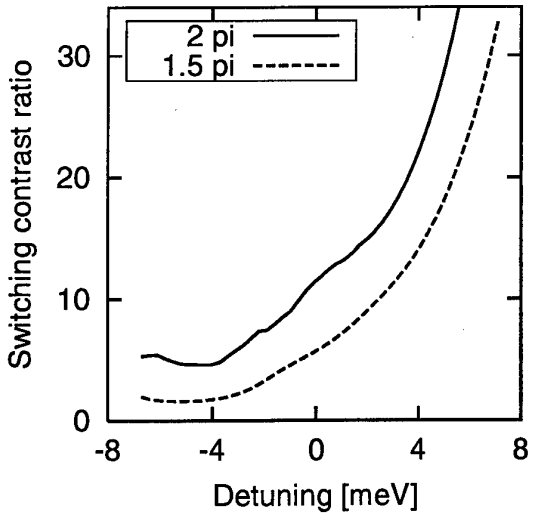

FIG. 11. Switching contrast ratio vs. detuning from the exciton resonance for InGaAs/InAlAs MQW NLDC with two different input pulse areas: 2π (solid line) and 1.5π (dashed line).

Task 4. New design of broadly tunable devices for WDM applications

In the new device design, the constituent waveguides of the resonant soliton NLDC are to be fabricated from a semiconductor quantum-dot-doped glass. Semiconductor quantum dots (QDs) are fascinating systems demonstrating three-dimensional quantum-confinement effects as the dot size approaches the exciton Bohr radius. This quantum confinement gives rise to interesting new properties, in particular, a strong enhancement of the excitonic nonlinear optical response.

The semiconductor material of interest for the new device design is PbS. There are two main reasons why PbS is attractive as the nanocrystallite material in QD-doped glasses. First, the small carrier effective masses ($m_e \approx m_h \approx 0.1m$) and large optical dielectric constant of PbS ($\epsilon = 17.2$) result in a large bulk exciton Bohr radius ($a_B = 18$ nm) allowing for strong confinement with relatively large nanocrystals [25,26]. Note that undesirable surface effects are reduced in larger QDs. Second, a spectral position of the excitonic resonance in PbS is in the range of interest for WDM systems. Due to a broad size distribution of the semiconductor QDs in glass matrix, a spectral width of the excitonic absorption band is typically very large. In the strong confinement regime, by changing the mean radius of QDs, large energy shifts of the absorption resonance can be achieved. Shown in Fig. 12 is the excitonic absorption spectrum of 4-nm PbS quantum dots in a glass matrix at room temperature [25]. This spectrum features a broad excitonic peak centered just below 1400 nm. For 7.5-nm PbS quantum dots in a glass matrix, a similar excitonic absorption peak is centered at about 1560 nm [26]. Therefore, by controlling the QD size, the device operating spectral range can be shifted up or down (see inset in Fig. 12).

Using the material parameters of the PbS QD-doped glass and adopting the mean QD raduis of 7.5 nm (the exciton resonance is at ~1560 nm) [26], the numerical simulations of operation of the resonant soliton NLDC have been performed. A duration of the input pulses in the simulations has been 100 fs, and the device throughput has been 2 Tbit/s. Only the detunings below the resonance have been considered. Plotted in Fig. 13 is a numerical dependence of the switching contrast ratio on detuning from the exciton resonance. The switching contrast ratio increases monotonically with an increase in the detuning value. A comparison between two plotted curves, corresponding to 2π and 1.5π input pulses, demonstrates that the switching contrast ratio is generally higher in the case of stronger pulses. The tunability range of the device extends roughly from $\delta = 0$ to $\delta = 32$ meV, leading to a spectral operating window of about 65 nm. This value is much larger than that for InGaAs/InAlAs MQW structures, and it can be further increased via routine device optimization. Therefore, it appears that PbS QD-doped glass NLDC has a potential to meet the specific tunability requirement applied by the use of the tellurite-based EDFAs (gain bandwidth of ~80 nm) in WDM transmission systems.

Semiconductor QD-doped glass represents a less expensive alternative to epitaxially grown semiconductors, however, there are technological challenges for its production, and the main one is a precise control of the QD size distribution. Another challenge is a fabrication of high-quality QD-doped glass waveguides. At present, practical applications of PbS QD-doped glasses are few and limited to intracavity saturable absorbers in various laser systems. To the best of our knowledge, there have been no devices yet utilizing glass waveguides doped with PbS QDs. Recently, a fabrication of high-quality CdS QD-doped glass waveguides has been reported (using the sol-gel and ion exchange methods) [27]. It appears that the deployment of

QD-doped glass waveguide devices will mostly depend on improvements in the control of QD size distribution and capabilities of the waveguide fabrication.

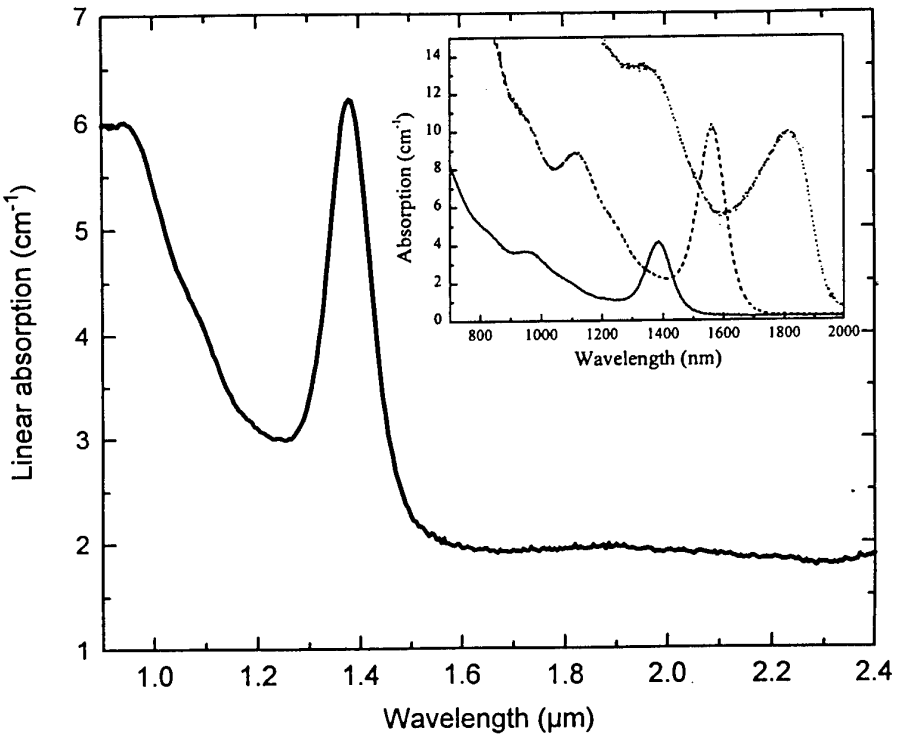

FIG. 12. Optical absorption spectrum of PbS QD-doped glass at room temperature. The exciton peak (about 63 meV FWHM) is centered at 1.38 μm and corresponds to an average dot radius of 4 nm (the experimental results are taken from Ref. [25]). The inset shows the absorption spectra of PbS QD-doped glass with three different QD sizes: 6.6 nm (solid line), 7.5 nm (dashed line), and 9.3 nm (dotted line) [26].

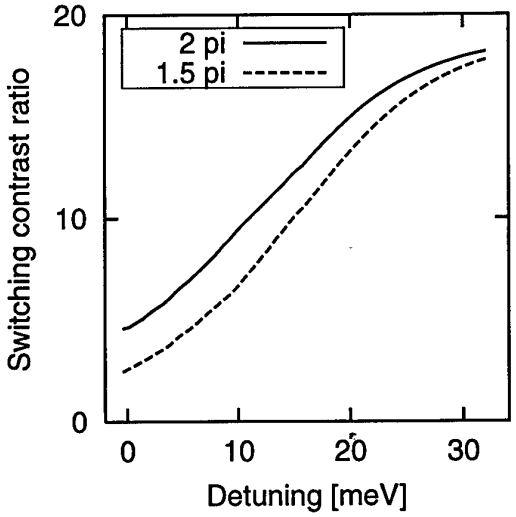

FIG. 13. Switching contrast ratio vs. detuning from the exciton resonance for PbS QD-doped glass NLDC with two different input pulse areas: 2π (solid line) and 1.5π (dashed line).

5. Summary

The following tasks have been completed in the research program performed during 1 July, 2000 – 31 December, 2000:

- **Task 1.**
  Numerical investigation of wavelength dependence (effects of detuning) and a possibility of tunable operation of the resonant soliton NLDC have been performed. A dramatic difference in the response to detuning between the semiconductor NLDC and an atomic SIT-soliton NLDC has been revealed; a physical reason for this difference has been discussed. Using II-VI semiconductor (CdZnTe/ZnTe MQW) material parameters, an operating spectral range of the resonant soliton NLDC of about 25 meV (~50 nm) and a mean switching contrast ratio of 20:1 within this range have been demonstrated numerically.

- **Task 2.**
  Extensive literature search has been performed to identify semiconductor materials which are suitable for implementation of the tunable resonant soliton switches operating near the optical communication wavelength (1.55 μm). A number of semiconductor systems with the required excitonic absorption features have been selected including InGaAs/InAlAs MQW, InGaNAs/GaAs MQW, InGaAs/InP MQW, InGaAsP/InP MQW and GaSb/AlGaSb MQW structures.

- **Task 3.**
  Modeling of operation of InGaAs/InAlAs MQW NLDC near 1.55 μm has been performed. A tunability range of about 12 meV (25 nm) and a mean switching contrast ratio of 20:1 within this range have been demonstrated numerically. A feasibility to meet the specific operating window requirement in WDM systems (applied by the gain bandwidth of erbium-doped fiber amplifiers) has been assessed.

- **Task 4.**
  A new device design has been suggested as a possible way to substantially increase the device tunability range. In the new design, semiconductor quantum-dot-doped glass has been used as a material for the constituent waveguides of NLDC. The use of PbS quantum dots has lead to a broader tunability range of, at least, 32 meV (~65 nm) of the device near 1.55 μm. Technological aspects of fabrication of semiconductor quantum-dot-doped glass waveguides have been discussed.

[1] N. Peyghambarian and I. Talanina, Final Technical Report, Grant No. F4962097-10180, AFOSR/NM (Program Manager: Dr. A. Nachman).
[2] I. Talanina, Final Technical Report, Contract F62562–98M9148, AOARD/AFOSR (Program Manager: Dr. M. Gaudreault).
[3] I. Talanina, Final Technical Report, Contract F62562–99M9105, AOARD/AFOSR (Program Manager: Dr. M. Gaudreault).
[4] C.D. Chen, I. Kim, O. Mizuhara, T.V. Nguyen, K. Ogawa, R.E. Tench, L.D. Tzeng and P.D. Yeates, Electron. Lett. **35**, 648 (1999).
[5] H. Omo, M. Yamada and Y. Ohishi, IEEE Photonics Technol. Lett. **9**, 596 (1997).
[6] M. Yamada, OFC '98, 1998, Paper PD7.
[7] S. Kawanishi, H. Takara, K. Uchiyama, I. Shake and K. Mori, Electron. Lett. **35**, 826 (1999).
[8] T. Ono and Y. Yano, IEEE J. Quantum Electron. **34**, 2080 (1998).
[9] I. Talanina, D. Burak, R. Binder, H. Giessen, and N. Peyghambarian, Phys. Rev. E **58**, 1074 (1998); I. Talanina, Phys. Lett. A **241**, 179 (1998).
[10] A. Guzman, F. S. Locati, M. Romagnoli, and S. Wabnitz, Phys. Rev. A **46**, 1594 (1992).
[11] I.B. Talanina, M.A. Collins, and V.M. Agranovich, Solid State Commun. **88**, 541 (1993); *ibid.*, in "Confined Electrons and Photons: New Physics and Devices" (Edited by C. Weisbuch), Plenum, New York (1995); I.B. Talanina, Solid State Commun. **97**, 273 (1996).
[12] P.C. Becker, D. Lee, M.R.X. de Barros, A.M. Johnson, A.G. Prosser, R.D. Feldman, R.F. Austin, and R.E. Behringer, IEEE J. Quant. Electr. **28**, 2535 (1992).
[13] Y. Kawamura, K. Wakita, and H. Asahi, Electron. Lett. **21**, 1168 (1985).
[14] J.S. Weiner, D.S. Chemla, D.A.B. Miller, T.H. Wood, D. Sivco, and A.Y. Cho, Appl. Phys. Lett. **46**, 619 (1985).
[15] H. Asai and Y. Kawamura, Appl. Phys. Lett. **56**, 746 (1990).
[16] H. Kobayashi, R. Takahashi, Y. Matsuoka and H. Iwamura, Electron. Lett. **34**, 908 (1998).
[17] R. Takahashi, Y. Kawamura and H. Iwamura, Appl. Phys. Lett. **68**, 153 (1996).
[18] Y. Kawaguchi and H. Asahi, Appl. Phys. Lett. **50**, 1243 (1987).
[19] M. Kondow, K. Uomi, A. Niwa, T. Kitatani, S. Watahiki and Y. Yazawa, Jpn. J. Appl. Phys. **35**, 1273 (1996).
[20] M. Kondow, T. Kitatani, S. Nakatsuka, MC. Larson, K. Nakahara, Y. Yazawa, M. Okai and K. Uomi, IEEE J. Selec. Topics Quantum. Electron. **3**, 719 (1997).
[21] T. Miyamoto, K. Takeuchi, T. Kageyama, F. Koyama and K. Iga, Jpn. J. Appl. Phys. **37**, 90 (1998).
[22] J. Hader, S.W. Koch, J.V. Moloney and E.P. O'Reilly, Appl. Phys. Lett. **77**, 630 (2000).
[23] W. Kowalsky, H.H. Wehmann, F. Fiedler, and A. Schlachetzki, Phys. Stat. Sol. (a) **77**, K75 (1983).
[24] T. Miyazawa, S. Tarucha, Y. Ohmori, Y. Suzuki and H. Okamoto, Jpn. J. Appl. Phys. **25**, L200 (1986).
[25] J. Butty, G.E. Jabbour, H. Tajalli, N. Peyghambarian, and N.F. Borrelli, *Absorption saturation in PbS quantum dots*, Internal report, Optical Sciences Center, University of Arizona, 1997.
[26] P.T. Guerreiro, S. Ten, N.F. Borrelli, J. Butty, G.E. Jabbour and N. Peyghambarian, Appl. Phys. Lett. **71**, 1595 (1997).
[27] S.G. Lee , K.I. Kang, P. Guerreiro, N. Peyghambarian, S.I. Najafi, G. Zhang, Y.H. Kao, C.Y. Li, T. Takada and J. Mackenzie, *Femtosecond pulse propagation in a cadmium sulfide semiconductor quantum dot waveguide*, CLEO '94 Technical Digest Series, Vol. 8, p. 85.